J. Phys. IV France 11 (2001)

Peculiarities of the martensitic transformation in ZrCu intermetallic compound – potential high temperature SMA

G.S. Firstov, J. Van Humbeeck and Yu.N. Koval[1]

Katholieke Universiteit Leuven, de Croylaan 2, 3001 Leuven, Heverlee, Belgium
[1] *Institute of Metal Physics of the National Academy of Sciences of Ukraine, 36 Vernadsky Str., 03142 Kiev 142, Ukraine*

Abstract. Interaction of two martensitic phases during martensitic transformation (MT) in ZrCu intermetallic compound was studied by means of *in situ* high-temperature X-ray diffraction studies, internal friction and calorimetric measurements. Some regularities of the mutual formation and disappearance of two martensites on thermal cycling through the temperature interval of the MT were established. The mechanism of the MT in ZrCu intermetallic compounds is discussed.

1. INTRODUCTION

It is known that the ZrCu-based intermetallic compounds undergo a martensitic transformation (MT) with wide temperature hysteresis and a considerable energy is dissipated during a full transformation cycle [1-3]. It has been shown that these intermetallics exhibit perfect shape memory effect [1,2,4] during MT with wide temperature hysteresis from high-temperature B2 phase into two monoclinic phases belonging to Cm and $P2_1/m$ space groups [5]. The process of the actual formation and disappearance of two martensites and austenite during the complete cycle of the MT in ZrCu intermetallic compound is a subject of the present investigation.

2. EXPERIMENTAL

The Zr-49.9 at.% Cu (ZrCu) alloy used in this investigation was arc-melted from iodide zirconium and electrolytic copper in an argon atmosphere, poured into water cooled copper mold and then quenched into water from 800°C. Its good homogeneity was confirmed by X-ray microanalysis (JCXA-733). MT heats and temperatures were detected by TA 2920 differential scanning calorimeter in the −100°C ↔ 450°C temperature range. Then calorimetric peaks were analyzed with the help of the PeakFit 4.06 software package employing distorted Pearson IV function. Internal friction measurements (IF) in −100°C ↔ 450°C temperature range were performed using DMA TA-983 apparatus. IF measurements in 25°C ↔ 400°C temperature range were performed also by means of the impulse excitation technique (IET) that determines the internal friction from the exponential decay of the amplitude of the vibration of a specimen after a light impact. An IET device (RFDA, IMCE) described in [6] was used to investigate plate-shaped specimens (nominal size 40x4x1 mm^3 and weight 1g) suspended in the nodes of their first bending vibration mode. The Young's moduli are calculated from the bending resonance frequency f_r according to ASTM C 1259-94. The internal friction Q^{-1} is calculated as $Q^{-1}=k/(\pi f_r)$ with k the exponential decay parameter of the bending mode component [7]. Crystal structure analysis as performed using *in situ* high temperature X-ray diffractometry (Seifert 3003 TT, HDK 2.4 furnace, Cu-K_α) and Rietveld refinement (DBWS 9006PC program - new version [8]). Volume fractions of the observed phases were derived from the results of the Rietveld refinement according to [9]. Volume changes during MT were determined using Du Pont TMA 934 dilatometer.

3. RESULTS AND DISCUSSION

The results of the dynamic mechanical response measurements on the second complete MT cycle in ZrCu are presented in Fig. 1. The plate specimen was loaded in parent phase in a way that strain amplitude was equal to about 10^{-3}. It is seen that the low frequency elastic modulus increases linearly on cooling from 300°C until 160°C. Then it starts to decrease and after passing a minimum around 80°C increases again until -50°C. IF dependence during this cooling shows a broad maximum clearly containing at least two peaks and correlates with a modulus decrease. Further cooling to -50°C reveals a small peak around 0°C. Subsequent heating results in a decrease of the

low frequency modulus with a minimum at 310°C with further two step increase that finishes at 370°C. The correspondent IF dependence shows a weak maximum at 50°C and a maximum at 310°C with a prolonged completion.

The elastic modulus and the internal friction on the second complete MT cycle in ZrCu measured by the impulse excitation technique are shown in Fig. 2. Both properties are showing approximately the same behaviour as for the dynamic mechanical response measurements presented in Fig. 1. High frequency elastic modulus behaviour has almost the same magnitude and differs only in a slope of its general increase on cooling. IF is significantly lower in this case, especially above 200°C. IF peak on cooling (Fig. 2, closed triangles) correlates well with the DMA one (Fig. 1) but starts higher – at 220°C. Then the small peak slightly above 50°C can be seen also. On subsequent heating the high frequency elastic modulus (Fig. 2, open circles) shows a minimum around 280°C that is lower in temperature and smaller in magnitude than the DMA one (Fig. 1). Correspondent IF peak on heating (Fig. 2, open triangles) is very weak. The difference in absolute values in results of DMA and IET measurements is related to the large difference in strain amplitude (10^{-7} for IET that is 10^4 times smaller than for DMA).

The results of the DSC measurements are presented in Fig. 3. The second forward MT exothermic reaction starts at 170°C and finishes around 30°C after passing two maximums. The second reverse MT endothermic reaction starts at 280°C and finishes at 420°C after passing two maximums as well. The general amount of the released heat on the forward MT was equal to $\mathbf{Q^{A>M}=977\ J/mol}$ (12.63 J/g) and for the reverse MT it was equal to $\mathbf{Q^{M>A}=1345\ J/mol}$ (17.38 J/g). These general two step peaks were fitted with the help of the two distorted Pearson peak functions each and as a result we were able to obtain the transformation heats and temperatures for each step as it is shown in Fig. 3.

Knowing already a presence of two martensitic phases (Cm and B19`) as a result of MT in ZrCu [5] it was obvious to perform *in situ* high temperature X-ray diffraction measurements in order to bring into correlation structural parameters of all the present phases and there order of appearance with the obtained heats and temperatures of the extracted intrinsic MT steps.

In particular, the Rietveld refinement of X-ray diffraction patterns obtained on cooling and heating during complete MT cycle in ZrCu allowed us to obtain the temperature dependencies of the volume fractions for all phases present as well as changes in there lattice parameters. The results of this analysis are shown in Fig. 4 and 5. It is seen how B2 volume fraction (Fig. 4, open boxes) starts to decrease on cooling at 170°C up to around room temperature correspondingly to the overall exothermic reaction (Fig. 3). At the same time, the volume fractions of the B19` martensite (Fig. 4, closed triangles) and of the martensite belonging to the Cm space group (Fig. 4, open circles) increase in amount. It is impossible to recognize which type of martensite forms first but it is clearly seen that B19` martensite finishes its appearance around 100°C, while martensite belonging to the Cm space group proceeds to form until about 30°C, replacing austenite completely. It means that the first sharp intrinsic exothermic peak was caused by the formation of the B19` martensite (Fig. 3). Taking into account its volume fraction (23%) and the amount of heat of the first sharp exothermic peak extracted after fitting (343 J/mol) we are able to find the heat of the imaginary separate forward B2>B19` MT in ZrCu $\mathbf{Q^{B2>B19`}=1490\ J/mol}$. The same can be done for the prolonged intrinsic exothermic peak that is attributed to the imaginary separate forward B2→Cm MT in ZrCu - $\mathbf{Q^{B2>Cm}=823\ J/mol}$ . Further heating leads to the appearance of the B2 austenite around 250°C which starts to replace B19` martensite first and corresponds to the sharp peak of the first intrinsic endothermic reaction that finishes around 350°C . The volume fraction of the Cm martensite starts to decrease at 300°C that correlates well with the beginning of the second intrinsic endothermic reaction which is prolonged until approximately 420°C . Again, we are able to obtain MT heats for both reverse intrinsic MT`s . So, $\mathbf{Q^{B19`>B2}=2030\ J/mol}$ and $\mathbf{Q^{Cm>B2}=1140\ J/mol}$. According to Ortin and Planes [10], the difference between reverse and forward MT heats represents the amount of energy dissipated during the complete MT cycle $\mathbf{Ed=Q^{M>A}-Q^{A>M}}$. For the second cycle of MT for ZrCu in general this dissipated energy will be $\mathbf{E_d^{ZrCu} = 1345 - 977 = 368\ J/mol}$. For the imaginary distinct B2<>B19` and B2<>Cm MT`s those dissipated energies will be, $\mathbf{E_d^{B2\leftrightarrow B19`} = 2030 - 1491 = 539\ J/mol}$ and $\mathbf{E_d^{B2\leftrightarrow Cm} = 1140 - 823 = 317\ J/mol}$. It is seen that the actual dissipated energy is almost the same in amount as the possible energy loss for the imaginary distinct B2<>Cm MT. The Rietveld refinement helped us to retrieve the lattice parameters for all the observed phases, also. Temperature dependencies of those lattice parameters are represented in Fig. 5. B2 phase lattice parameter decreases on cooling (and increases on heating) can be simply approximated by the following linear function: $\mathbf{a_{B2}=3.261_8+T\cdot5\cdot10^{-5}}$ Å (Fig. 5 (a), T-temperature,°C). Parameter $\mathbf{a_{B19`}}$ increases on cooling (decreases on heating) - $\mathbf{a_{B19`}=3.283_6-T\cdot6\cdot10^{-5}}$ Å. It should be noted that their temperature dependencies cross each other around 200°C that is slightly above M_s for this complete MT cycle in ZrCu (Fig. 5 (a)). Parameter $\mathbf{b_{B19`}}$ increases almost linearly on heating ($\mathbf{b_{B19`}=4.178_7+T\cdot10^{-4}}$ Å), while $\mathbf{c_{B19`}}$ has a maximum at a

350°C as well as monoclinic angle $\beta_{B19'}$ which decreases on heating (Fig. 5 (b)). This maximum corresponds to $A_{fl} = A_f^{B19' \rightarrow B2}$ temperature. Lattice parameters c_{Cm} and β_{Cm} behaviour is very similar to that in B19` martensite, only the peak on heating can be observed around 300°C (Fig. 5 (b,c)). As for the a_{Cm} and b_{Cm}, they show the same behaviour on heating (slight increase; Fig. 5 (c)) but on cooling b_{Cm} undergoes a decrease, while a_{Cm} increases.

Then, the lattice parameters of the austenite and both martensites were used to calculate the volume per atom changes during B2<>B19` and B2<>Cm MT`s (Fig. 5 (d)). Calculated volume effect for both forward MT`s is positive and in the 0.2-0.3% range. Linear approximations of such volume effect temperature dependencies tell us that the B2>B19` forward MT volume effect is bigger than for B2>Cm MT in ZrCu. It can be also clearly seen that calculated (Fig. 5 (d)) and observed volume changes during second MT (Fig. 6) are very close to each other.

The results stated above give us the possibility to explain the martensites` formation mechanism in ZrCu. According to the martensites` volume fraction change (Fig. 4) and DSC measurements (Fig. 3) it seems like the B19` martensite forms first preferentially. On the other hand, the structural analysis shows that the positive volume effect on forward MT for B19` is bigger than for Cm martensite (Fig. 5 (d)). Taking into account the results of Seo and Schryvers [11] that show alternate B19`→Cm→B19`→... "sandwich"-type of microstructure, it is logical to suppose that the formation of B19` martensite at first induces considerable stresses in surrounding matrix and the Cm martensite then forms as a relaxation of such stresses. Such forward MT can prevent the plastic deformation and can be the reason for the nearly perfect shape memory effect during MT in ZrCu that is taking place with wide temperature hysteresis [1]. The reverse MT shows that B19` martensite disappears first (Fig. 3,4). It indicates that MT in ZrCu is non-thermoelastic. The thermoelasticity concept that was confirmed experimentally [12] includes such requirement that the last portions of martensite phase on forward MT must be transformed to austenite in a first order. In ZrCu we have a completely opposite situation. Such order of appearance↔disappearance for the martensites in ZrCu can be also the reason for the more intensive energy dissipation as a result of serious overheating through B19` martensite "barrier" for B2↔Cm MT.

The most important question in this case, why B19` martensite forms first in spite of its bigger MT volume effect, twinless substructure etc.? In [5] the lattice correspondence between B2 and B19` for ZrCu was supposed as [100]B2 // [100]M , (011)B2 // (001)M , (011)B2 // (010)M. Lattice parameters $a_{B19'}$, and a_{B2} behaviour (Fig. 5 (a)) shows that their perfect match close to Ms can favor the formation of B19` at first on cooling.

CONCLUSIONS

- MT in ZrCu is of non-thermoelastic type.
- The relaxation of internal elastic stresses during forward B2>B19` MT in ZrCu takes place by means of the formation of additional Cm martensite instead of twinning or plastic deformation.
- The perfect match of the interplanar spacings of the (100) parallel planes for B2 and B19` phases can be the reason for the initial formation of the B19` martensite.

References

[1] Koval Yu.N., Firstov G.S., Kotko A.V., *Scripta Met. et Mat.*,**27**, (1992) pp. 1611-1616.

[2] Koval Yu.N., Firstov G.S., Van Humbeeck J., Delaey L., Jang W.Y., "B2 intermetallic compounds of Zr. New class of the shape memory alloys", Proc. of the ICOMAT-95, Lausanne 20-25 August 1995, Switzerland, R.Gotthardt and J. Van Humbeeck Eds., *J. Physique IV*, C8, **5**, (Les Editions de Physique, 1995) pp. 1103-1108.

[3] Firstov G.S., Koval Yu.N., Van Humbeeck J., "Irreversible processes during martensitic transformation in Zr-based shape memory alloys", Proc. of the ESOMAT`97, Enschede 1-5 July 1997, The Netherlands, J.Beyer, A. Böttger and J.H. Mulder Eds., *J. Physique IV*, C5, **7**, (1997) pp.549-554.

[4] Firstov G.S., Koval Yu.N., Van Humbeeck J., "Shape memory behaviour in quasibinary ZrCu-based intermetallic compounds", Proc. of the SMST`99, Antwerp Zoo 5-9 September 1999, Belgium, to be published.

[5] Schryvers D., Firstov G.S., Seo J.W., Van Humbeeck J., Koval Yu.N., *Scripta Mat.*,**36**, (1997) pp.1119-1125.

[6] Roebben G., Bollen B., Brebels A., Van Humbeeck J., Van der Biest O., *Rev. scient. Instrum.*, 1997, **68**, pp.4511-4515.

[7] Nowick A.S., Berry B.S., in *Anelastic Relaxation in Crystalline Solids*, Academic Press, New York, 1972.

[8] Wiles D.B., Young R.A., *J. Appl. Cryst.*,**14**, (1981) pp. 149-151.

[9] Hill R.J., Howard C.J., *J. Appl. Cryst.*, **20**, (1987) pp. 467-481.

[10] Ortin J., Planes A., *Acta Metall.*, **36**, No.8, (1988) pp. 1873-1889.

[11] Seo J.W., Schryvers D., *Acta mater.*, 46, No. 4, (1998), pp. 1165-1175.

[12] G.V. Kurdjumov, L.G. Khandros, *Doklady Akad. Nauk SSSR*, **66**, (1949) pp. 211-221.

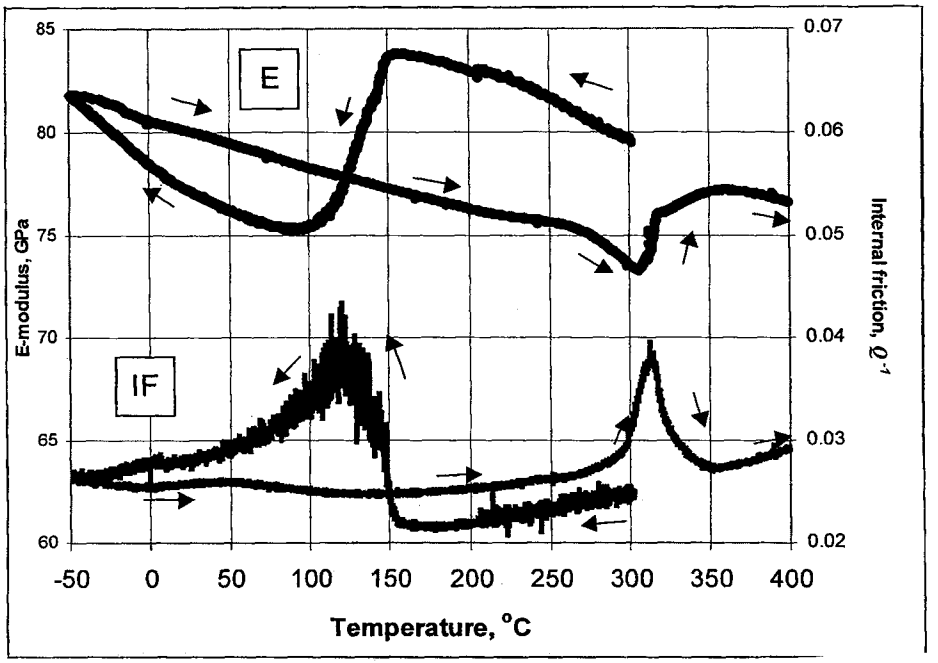

Figure 1: Evolution of the internal friction (IF) and modulus (E) during the second complete MT cycle in ZrCu (5°C/min, DMA – fixed frequency 4 Hz, $\approx 10^{-3}$ strain amplitude).

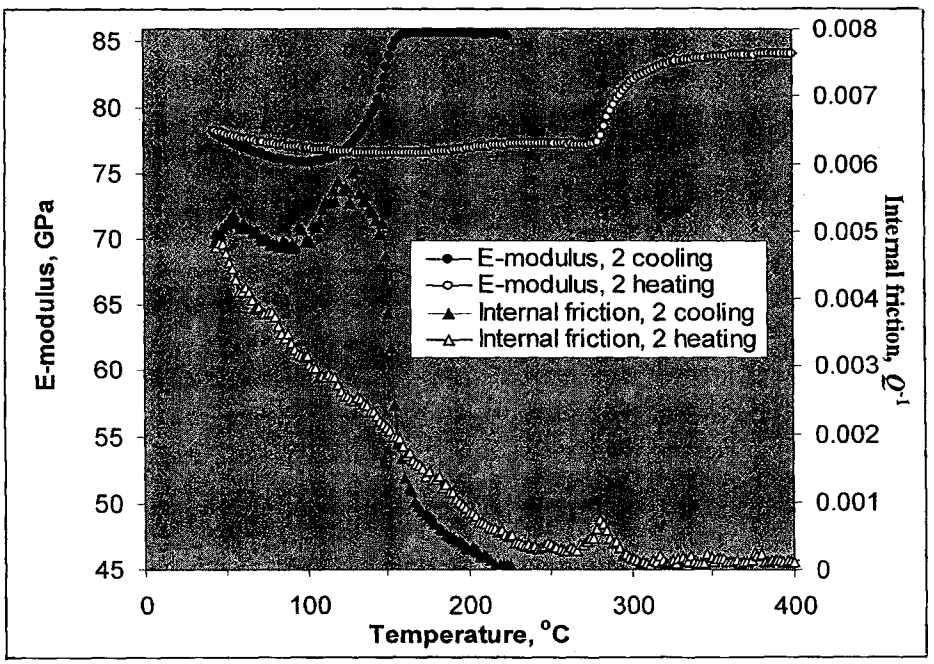

Figure 2: Evolution of the internal friction and E-modulus during the second complete MT cycle in ZrCu (5°C/min, IET, $fr \approx 4.2$-4.4 kHz, $\approx 10^{-7}$ strain amplitude)

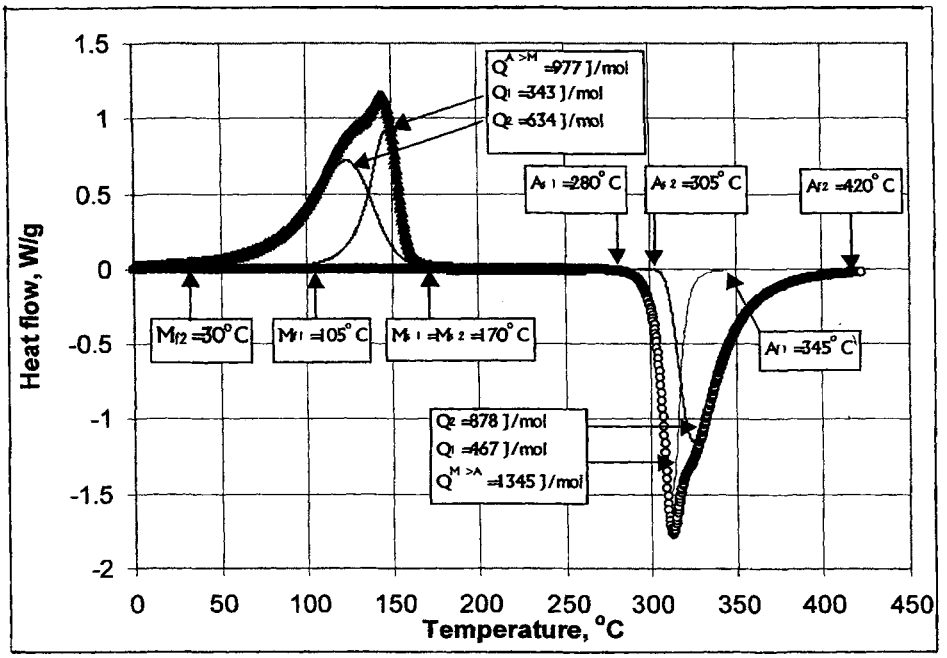

Figure 3: DSC measurement results of the second complete MT cycle in ZrCu (10°C/min)

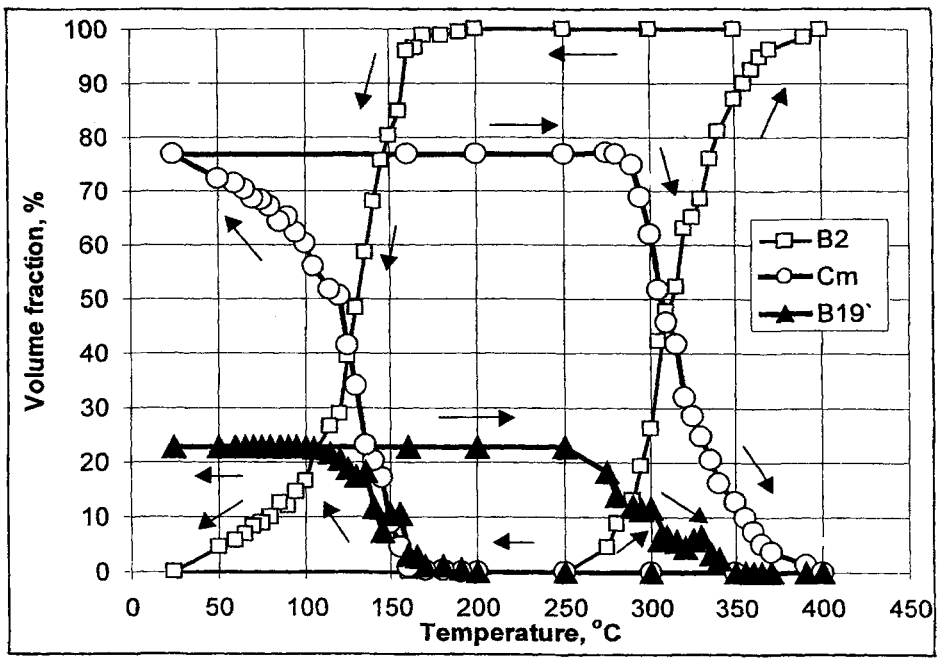

Figure 4: Changes in the volume fractions for B2, Cm and B19` phases derived from the results of the Rietveld refinement of the X-ray diffraction patterns taken on cooling-heating cycle during the second MT in ZrCu.

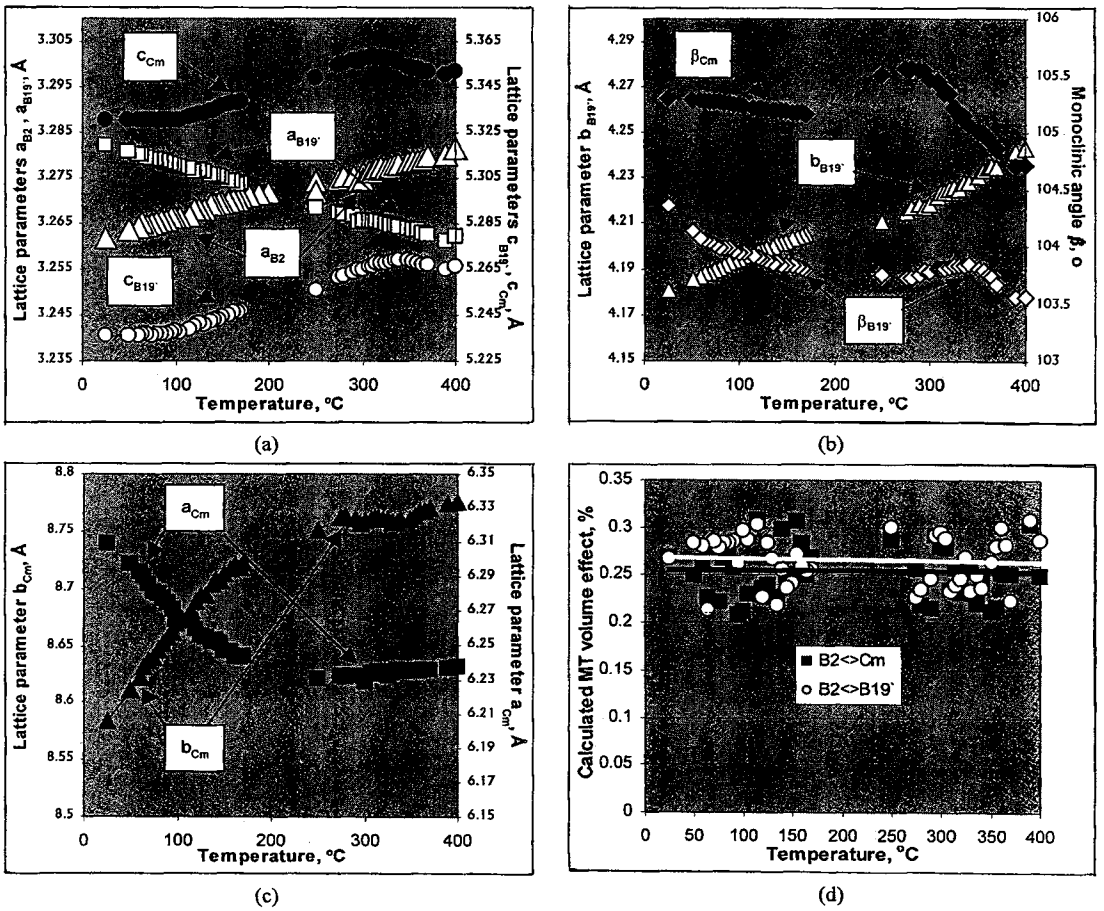

Figure 5: Lattice parameters changes for B2 (c), Cm (a,b,c) and B19`(b,c) phases derived from the results of the Rietveld refinement of the X-ray diffraction patterns taken on cooling-heating cycle during second MT in ZrCu and MT volume effect calculated from relation between the lattice parameters of the austenite and both martensites (d).

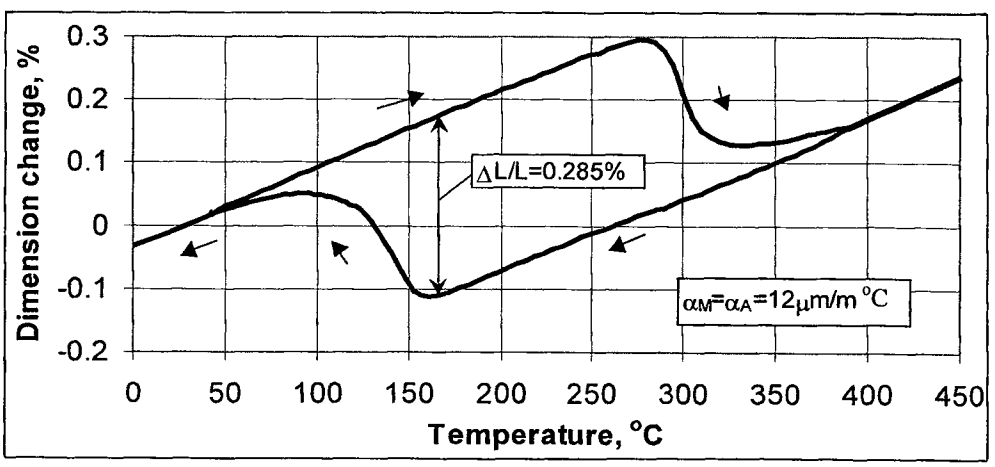

Figure 6: Dilatometric measurements of the second complete MT cycle in ZrCu